定子开槽表贴式永磁电机转子偏心空载气隙磁场全局解析法

李　琛，章跃进，周晓燕，仇志坚

(上海大学 机电工程与自动化学院，上海 200072)

摘　要：本文基于正则摄动理论，计及定子开槽，建立了表贴式永磁电机转子偏心全局解析模型。采用全局解析法，将解析区域划分为永磁体、气隙和槽区域，通过各子区域之间的边界条件，求解拉普拉斯方程或泊松方程。偏心气隙磁密由零阶分量和一阶分量组成。气隙磁密、齿槽转矩和不平衡磁拉力的解析解与有限元解趋于一致，验证了解析模型的合理性。

关键词：表贴式；定子开槽；转子偏心；空载气隙磁场；全局解析法

Exact Analytical Solution of Open-circuit Air-gap Magnetic Field in Slotted Surface-mounted Permanent-magnet Motors with Rotor Eccentricity

Li Chen, Zhang Yue-jin, Zhou Xiao-yan, Qiu Zhi-jian

(School of Mechatronics Engineering and Automation, Shanghai University, Shanghai, 200072)

ABSTRACT: An exact analytical model for the air-gap magnetic field predicting in slotted surface-mounted permanent-magnet motor with rotor eccentricity was established in this paper, based on the applying of the perturbation method. The magnetic field domain is divided into three subdomains, viz. magnet, air-gap and slots. The analytical solution is derived by solving the Laplace's or Poisson's equations with the boundary conditions to the interfaces between these subdomains applied. The air-gap flux density with rotor eccentricity is consists of zero-order components and first-order components. The air-gap flux density, cogging torque and unbalanced magnetic forces were computed. The analytical results remain the same trend of the finite-element analysis (FEA) results. As a result, the rationality of the analytical model was verified

KEY WORDS: surface-mounted; slotted; rotor eccentricity; open-circuit magnetic field; exact analytical solution

0　引言

转子偏心，即永磁电机在装配和运行过程中，出现的定、转子不同心的情况。它所产生的不平衡磁拉力，是引起永磁电机振动、噪声和转矩脉动的原因之一。

为研究永磁电机转子偏心对电机性能的影响，可采用有限元法或解析法，获取偏心气隙磁场分布。有限元法适应性强，精度高，几何模型和材料属性的准确度高，但是建模复杂，计算耗时较长；解析法有一定的假设条件，模型比较单一，但参数调整方便，计算迅速。

许多学者采用解析法计算表贴式永磁电机转子偏心气隙磁场，并取得了一定的研究成果。Kim在文献[1]中，首次将正则摄动理论运用到表贴式永磁电机偏心气隙磁场解析中，文中采用标量磁位计算，转子永磁体径向充磁；文献[2]分别分析了多种永磁体充磁方式下，内、外转子永磁电机的偏心气隙磁场分布和不平衡磁拉力。文献[3]采用矢量磁位求解，解析模型中的偏心扰动量无量纲。以上文献中均为定子无槽模型，工程应用价值受限。

文献[4]采用等效剩磁法，将偏心后的不均匀气隙，等效为不均匀永磁体，并采用比磁导函数修正开槽后气隙磁密的径向分量，由于切向分量被隐没，故无法准确计算不平衡磁拉力；文献[5-6]通过对偏心边值问题的二次处理，模拟定子开槽，但此方法的计算精度不够高；文献[7]采用保角变换法，引入复数比磁导函数，实部和虚部分别修正气隙磁密的径向和切向分量，但该模型将定子槽等效为无限深的单槽结构，无法考虑槽与槽之间的影响；文献[8]采用全局解析法，以标量磁位计算偏心气隙磁场分布，每个槽就是一个子区域，计及槽与槽的相互影响，但其解析表达式中的待定系数，以离散值的形式出现，并无完整表达式。

本文建立了定子开槽表贴式永磁电机转子偏心空载气隙磁场全局解析模型，采用矢量磁位计算

磁场分布，由于矢量磁位适合于有电流区域，为后续研究中叠加电枢反应磁场提供便利。通过建立有限元分析模型，将气隙磁密、齿槽转矩和不平衡磁拉力的解析解与有限元解相比较，验证解析模型的合理性。

1　转子偏心解析模型

1.1 转子偏心数学模型

为便于数学建模，做如下假设：

1) 二维极坐标系计算，忽略饱和效应；

2) 永磁体线性退磁，相对磁导率 $\mu_r=1$；

3) 定、转子铁芯磁导率无穷大；

4) 定子扇形槽。

转子偏心解析模型如图 1 所示。解析区域被划分为：永磁区域 1、气隙区域 2 和槽区域 3i(i=1,2,⋯Q)，Q 为定子槽数。R_{sy} 为定子槽底半径、R_s 为定子内半径、R_m 为永磁体半径、R_r 为转子半径，β 为槽口角度，$\theta_i=-\beta/2+i2\pi/Q$ 为第 i 槽初始角度。

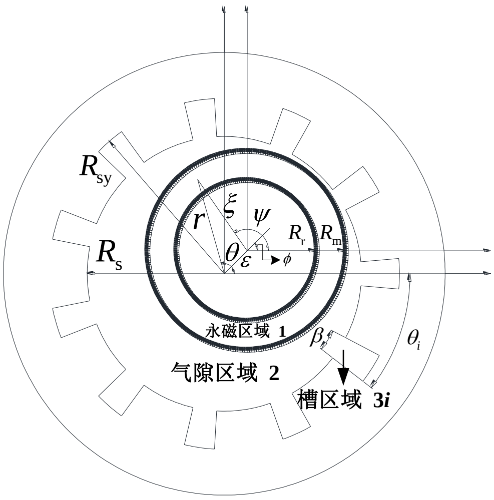

图 1 转子偏心解析模型

Fig.1 Analytical model with rotor eccentricity

图中，分别以转子圆心和定子圆心为原点，建立转子坐标系 ξ-ψ 和定子坐标系 r-θ，两坐标原点之间线段的长度，被定义为偏心量 ε。转子坐标系偏离定子坐标系的角度，被定义为偏心角度 ϕ。

通过几何变换，可得两坐标系之间的关系为[1]：

$$r=\xi+\varepsilon\cos(\theta-\phi)+\mathrm{O}(\varepsilon^2) \tag{1}$$

$$\psi-\psi_0=\theta-\theta_0+\frac{\varepsilon}{r}\sin(\theta-\phi)+\mathrm{O}(\varepsilon^2) \tag{2}$$

其中，$\mathrm{O}(\varepsilon^2)$ 为偏心量 ε 的高阶无穷小，ψ_0 和 θ_0 分别为转子坐标系和定子坐标系下，永磁体的初始角度。

1.2 永磁体磁化强度表达式

在转子坐标系 ξ-ψ 中，永磁体对称分布，径向充磁方式下，其磁化强度的傅立叶展开式为[9]：

$$\begin{cases} M_\xi(\psi)=\sum\limits_{n=1,3,5...}^{\infty} M_n\cos nm(\psi-\psi_0) \\ M_\psi(\psi)=0 \end{cases} \tag{3}$$

其中，$M_\xi(\psi)$ 和 $M_\psi(\psi)$ 分别为转子坐标系下，永磁体磁化强度的径向和切向分量，$M_n=4B_r\cdot\sin(n\pi\alpha_p/2)/\mu_0 n\pi$，$B_r$ 为永磁体剩磁，p 为极对数，m 为 p 和 Q 的最大公约数，α_p 为极弧系数，μ_0 为空气磁导率，n=1,3,5,…为永磁体磁化强度傅立叶展开次数。

根据式(2)(3)，考虑到 ε 为极小量，视之为零，则定子坐标系 r-θ 中，永磁体磁化强度表达式为[8]：

$$\mathbf{M}=M_r(\theta)\cdot\mathbf{r}+M_\theta(\theta)\cdot\boldsymbol{\theta} \tag{4}$$

$$\begin{cases} M_r(\theta)=\sum\limits_{n=1,3,5...}^{\infty} M_n\cos nm(\theta-\theta_0) \\ M_\theta(\theta)=0 \end{cases} \tag{5}$$

其中，$M_r(\theta)$ 和 $M_\theta(\theta)$ 分别为定子坐标系下，永磁体磁化强度的径向和切向分量。

1.3 正则摄动偏心边界条件

根据正则摄动理论，各解析区域内的矢量磁位、磁场强度、磁通密度可表示为[1]：

$$A(r,\theta,\varepsilon)=A^{(0)}(r,\theta)+\varepsilon A^{(1)}(r,\theta)+\mathrm{O}(\varepsilon^2) \tag{6}$$

$$H(r,\theta,\varepsilon)=H^{(0)}(r,\theta)+\varepsilon H^{(1)}(r,\theta)+\mathrm{O}(\varepsilon^2) \tag{7}$$

$$B(r,\theta,\varepsilon)=B^{(0)}(r,\theta)+\varepsilon B^{(1)}(r,\theta)+\mathrm{O}(\varepsilon^2) \tag{8}$$

其中，上标(0)和(1)分别代表相应变量的零阶分量和一阶分量。

各区域内磁通密度和磁场强度的关系为：

$$\begin{cases} B_1=\mu_0(\mu_r H_1+M) \\ B_2=\mu_0 H_2 \\ B_{3,i}=\mu_0 H_{3,i} \end{cases} \tag{9}$$

其中，下标表示相应的解析区域。

由矢量磁位求取各区域磁通密度的径向分量和切向分量分别为：

$$\begin{cases} B_r=\dfrac{1}{r}\dfrac{\partial A(r,\theta)}{\partial\theta} \\ B_\theta=-\dfrac{\partial A(r,\theta)}{\partial r} \end{cases} \tag{10}$$

转子和永磁体交界处、永磁体和气隙交界处，

边界的法向量可分别表示为：

$$\mathbf{n}_{rotor-mag}(r,\theta,\varepsilon)=\mathbf{e}_r+\frac{\varepsilon}{r}\sin(\theta-\phi)\mathbf{e}_\theta+\mathrm{O}(\varepsilon^2) \tag{11}$$

$$\mathbf{n}_{mag-air}(r,\theta,\varepsilon)=\mathbf{e}_r+\frac{\varepsilon}{r}\sin(\theta-\phi)\mathbf{e}_\theta+\mathrm{O}(\varepsilon^2) \tag{12}$$

其中，$\mathbf{e}_r$ 和 $\mathbf{e}_\theta$ 分别为定子坐标系中的径向和切向单位向量。

那么，转子和永磁体交界处、永磁体和气隙交界处的边界条件，可描述为：

$$\mathbf{n}_{rotor-mag}\times H_1=0 \tag{13}$$

$$\mathbf{n}_{mag-air}\times(H_1-H_2)=0 \tag{14}$$

$$\mathbf{n}_{mag-air}\cdot(B_1-B_2)=0 \tag{15}$$

由(11)～(15)可得以下偏心摄动边界条件：

$$\begin{aligned}&H_{\theta 1}(r,\theta,\varepsilon)-\frac{\varepsilon}{r}\sin(\theta-\phi)\\&\cdot H_{r1}(r,\theta,\varepsilon)\ \Big|_{r=R_r+\varepsilon\cos(\theta-\phi)}=0\end{aligned} \tag{16}$$

$$\begin{aligned}&[H_{\theta 1}(r,\theta,\varepsilon)-H_{\theta 2}(r,\theta,\varepsilon)]-\frac{\varepsilon}{r}\sin(\theta-\phi)\\&\cdot[H_{r1}(r,\theta,\varepsilon)-H_{r2}(r,\theta,\varepsilon)]\ \Big|_{r=R_m+\varepsilon\cos(\theta-\phi)}=0\end{aligned} \tag{17}$$

$$\begin{aligned}&[B_{r1}(r,\theta,\varepsilon)-B_{r2}(r,\theta,\varepsilon)]+\frac{\varepsilon}{r}\sin(\theta-\phi)\\&\cdot[B_{\theta 1}(r,\theta,\varepsilon)-B_{\theta 2}(r,\theta,\varepsilon)]\ \Big|_{r=R_m+\varepsilon\cos(\theta-\phi)}=0\end{aligned} \tag{18}$$

其中，下标 r 和 θ 分别代表相应变量的径向和切向分量。

其余边界条件为：

$$\begin{cases}A_{3,i}(R_s,\theta,\varepsilon)=A_2(R_s,\theta,\varepsilon) & \theta\in[\theta_i,\theta_i+\beta]\\ H_{\theta 3,i}(R_s,\theta,\varepsilon)=H_{\theta 2}(R_s,\theta,\varepsilon) & \theta\in[\theta_i,\theta_i+\beta]\\ H_{\theta 3,i}(R_{sy},\theta,\varepsilon)=0 & \theta\in[\theta_i,\theta_i+\beta]\\ B_{r3,i}(r,\theta,\varepsilon)\big|_{\theta=\theta_i,\theta_i+\beta}=0 & r\in[R_s,R_{sy}]\end{cases} \tag{19}$$

将式(7)(9)(10)带入式(16)中，把式(16)在 $r=R_r$ 处泰勒展开：

$$-\frac{1}{\mu_0}\frac{\partial A_1^{(0)}(r,\theta)}{\partial r}\Bigg|_{r=R_r}-\varepsilon\left\{\begin{array}{l}\dfrac{1}{\mu_0}\dfrac{\partial A_1^{(1)}(r,\theta)}{\partial r}+\dfrac{1}{\mu_0 r^2}\sin(\theta-\phi)\dfrac{\partial A_1^{(0)}(r,\theta)}{\partial\theta}\\ -\dfrac{M_r(\theta)}{r}\sin(\theta-\phi)+\dfrac{\cos(\theta-\phi)}{\mu_0}\dfrac{\partial^2 A_1^{(0)}(r,\theta)}{\partial r^2}\end{array}\right\}\Bigg|_{r=R_r}=0 \tag{20}$$

将式(7)(9)(10)带入式(17)中，把式(17)在 $r=R_m$ 处泰勒展开：

$$-\frac{1}{\mu_0}\left[\frac{\partial A_1^{(0)}(r,\theta)}{\partial r}-\frac{\partial A_2^{(0)}(r,\theta)}{\partial r}\right]\Bigg|_{r=R_m}-\varepsilon\left\{\begin{array}{l}\dfrac{1}{\mu_0}\dfrac{\partial A_1^{(1)}(r,\theta)}{\partial r}-\dfrac{1}{\mu_0}\dfrac{\partial A_2^{(1)}(r,\theta)}{\partial r}\\ +\dfrac{1}{\mu_0 r^2}\sin(\theta-\phi)\left[\dfrac{\partial A_1^{(0)}(r,\theta)}{\partial\theta}-\dfrac{\partial A_2^{(0)}(r,\theta)}{\partial\theta}\right]\\ -\dfrac{M_r(\theta)}{r}\sin(\theta-\phi)\\ +\dfrac{\cos(\theta-\phi)}{\mu_0}\left[\dfrac{\partial^2 A_1^{(0)}(r,\theta)}{\partial r^2}-\dfrac{\partial^2 A_2^{(0)}(r,\theta)}{\partial r^2}\right]\end{array}\right\}\Bigg|_{r=R_m}=0 \tag{21}$$

将式(8)(9)(10)带入式(18)中，把式(18)在 $r=R_m$ 处泰勒展开：

$$\frac{1}{r}\left[\frac{\partial A_1^{(0)}(r,\theta)}{\partial\theta}-\frac{\partial A_2^{(0)}(r,\theta)}{\partial\theta}\right]\Bigg|_{r=R_m}+\varepsilon\left\{\begin{array}{l}\dfrac{1}{r}\left[\dfrac{\partial A_1^{(1)}(r,\theta)}{\partial\theta}-\dfrac{\partial A_2^{(1)}(r,\theta)}{\partial\theta}\right]\\ -\dfrac{\sin(\theta-\phi)}{r}\left[\dfrac{\partial A_1^{(0)}(r,\theta)}{\partial r}-\dfrac{\partial A_2^{(0)}(r,\theta)}{\partial r}\right]\\ -\dfrac{\cos(\theta-\phi)}{r^2}\left[\dfrac{\partial A_1^{(0)}(r,\theta)}{\partial\theta}-\dfrac{\partial A_2^{(0)}(r,\theta)}{\partial\theta}\right]\\ +\dfrac{\cos(\theta-\phi)}{r}\left[\dfrac{\partial^2 A_1^{(0)}(r,\theta)}{\partial\theta\partial r}-\dfrac{\partial^2 A_2^{(0)}(r,\theta)}{\partial\theta\partial r}\right]\end{array}\right\}\Bigg|_{r=R_m}=0 \tag{22}$$

2 零阶方程求解

2.1 零阶方程式

转子偏心后，各解析区域内矢量磁位的零阶分量满足零阶方程组[10]：

$$\begin{cases}\dfrac{\partial^2 A_1^{(0)}}{\partial r^2}+\dfrac{1}{r}\dfrac{\partial A_1^{(0)}}{\partial r}+\dfrac{1}{r^2}\dfrac{\partial^2 A_1^{(0)}}{\partial\theta^2}=-\mu_0\nabla\times\mathbf{M}\\ \dfrac{\partial^2 A_2^{(0)}}{\partial r^2}+\dfrac{1}{r}\dfrac{\partial A_2^{(0)}}{\partial r}+\dfrac{1}{r^2}\dfrac{\partial^2 A_2^{(0)}}{\partial\theta^2}=0\\ \dfrac{\partial^2 A_{3,i}^{(0)}}{\partial r^2}+\dfrac{1}{r}\dfrac{\partial A_{3,i}^{(0)}}{\partial r}+\dfrac{1}{r^2}\dfrac{\partial^2 A_{3,i}^{(0)}}{\partial\theta^2}=0\end{cases} \tag{23}$$

2.2 零阶方程边界条件

由式(19)~(22)可得零阶方程边界条件：

$$\begin{array}{ll}\dfrac{\partial A_1^{(0)}(R_r,\theta)}{\partial r}=0 & \\ \dfrac{\partial A_1^{(0)}(R_m,\theta)}{\partial r}-\dfrac{\partial A_2^{(0)}(R_m,\theta)}{\partial r}=0 & \\ \dfrac{\partial A_1^{(0)}(R_m,\theta)}{\partial\theta}-\dfrac{\partial A_2^{(0)}(R_m,\theta)}{\partial\theta}=0 & \\ A_{3,i}^{(0)}(R_s,\theta)=A_2^{(0)}(R_s,\theta) & \theta\in[\theta_i,\theta_i+\beta]\\ H_{\theta 3,i}^{(0)}(R_s,\theta)=H_{\theta 2}^{(0)}(R_s,\theta) & \theta\in[\theta_i,\theta_i+\beta]\\ H_{\theta 3,i}^{(0)}(R_{sy},\theta)=0 & \theta\in[\theta_i,\theta_i+\beta]\\ B_{r3,i}^{(0)}(r,\theta)\big|_{\theta=\theta_i,\theta_i+\beta}=0 & r\in[R_s,R_{sy}]\end{array} \tag{24}$$

2.3 矢量磁位零阶通式

永磁区域 1 内矢量磁位的零阶通式为：

$$A_1^{(0)}(r,\theta)=\sum_{n=1}^{\infty}\begin{bmatrix}(A_{1n}^{(0)}r^{nm}+B_{1n}^{(0)}r^{-nm})\cos nm\theta\\+(C_{1n}^{(0)}r^{nm}+D_{1n}^{(0)}r^{-nm})\sin nm\theta]\end{bmatrix}+\sum_{n=1,3,5}^{\infty}\mu_0 r\frac{nmM_n}{(nm)^2-1}\sin nm(\theta-\theta_0) \tag{25}$$

其中，n=1,2,…为永磁区域傅立叶展开次数，$A_{1n}^{(0)}\sim D_{1n}^{(0)}$为永磁区域零阶通解待定系数。

气隙区域 2 内矢量磁位的零阶通式为：

$$A_2^{(0)}(r,\theta)=\sum_{n=1}^{\infty}\begin{bmatrix}(A_{2n}^{(0)}r^{nm}+B_{2n}^{(0)}r^{-nm})\cos nm\theta\\+(C_{2n}^{(0)}r^{nm}+D_{2n}^{(0)}r^{-nm})\sin nm\theta]\end{bmatrix} \tag{26}$$

其中，n=1,2,…为气隙区域傅立叶展开次数，$A_{2n}^{(0)}\sim D_{2n}^{(0)}$为气隙区域零阶通解待定系数。

槽区域 3 内矢量磁位的零阶通式为：

$$A_{3,i}^{(0)}(r,\theta)=A_i^{(0)}+\sum_{k=1}^{\infty}A_{3,i}^{(0)}(k,i)\frac{(\frac{r}{R_{sy}})^{k\pi/\beta}+(\frac{r}{R_{sy}})^{-k\pi/\beta}}{(\frac{R_s}{R_{sy}})^{k\pi/\beta}+(\frac{R_s}{R_{sy}})^{-k\pi/\beta}}\cos\frac{k\pi}{\beta}(\theta-\theta_i) \tag{27}$$

其中，k=1,2,…为槽区域傅立叶展开次数，$A_i^{(0)}$和 $A_{3,i}^{(0)}(k,i)$ 为槽区域一阶通解待定系数。

联立以上零阶边界条件，求取各区域矢量磁位零阶通解待定系数后，根据式(10)可求得气隙磁密零阶分量。求解过程可参考文献[9]，此处不再赘述。

3 一阶方程求解

3.1 一阶方程式

转子偏心后，各解析区域内矢量磁位的一阶分量满足一阶方程组：

$$\begin{cases}\dfrac{\partial^2 A_1^{(1)}}{\partial r^2}+\dfrac{1}{r}\dfrac{\partial A_1^{(1)}}{\partial r}+\dfrac{1}{r^2}\dfrac{\partial^2 A_1^{(1)}}{\partial\theta^2}=0\\ \dfrac{\partial^2 A_2^{(1)}}{\partial r^2}+\dfrac{1}{r}\dfrac{\partial A_2^{(1)}}{\partial r}+\dfrac{1}{r^2}\dfrac{\partial^2 A_2^{(1)}}{\partial\theta^2}=0\\ \dfrac{\partial^2 A_{3,i}^{(1)}}{\partial r^2}+\dfrac{1}{r}\dfrac{\partial A_{3,i}^{(1)}}{\partial r}+\dfrac{1}{r^2}\dfrac{\partial^2 A_{3,i}^{(1)}}{\partial\theta^2}=0\end{cases} \tag{28}$$

3.2 一阶方程边界条件

由式(19)~(22)可得一阶方程边界条件：

$$\left.\frac{\partial A_1^{(1)}(r,\theta)}{\partial r}\right|_{r=R_r}=-\frac{\sin(\theta-\phi)}{R_r^{\ 2}}\left.\frac{\partial A_1^{(0)}(r,\theta)}{\partial\theta}\right|_{r=R_r}+\frac{\mu_0 M_r}{R_r}\sin(\theta-\phi)-\cos(\theta-\phi)\left.\frac{\partial^2 A_1^{(0)}(r,\theta)}{\partial r^2}\right|_{r=R_r} \tag{29}$$

$$\begin{aligned}&\left.\frac{\partial A_1^{(1)}(r,\theta)}{\partial r}-\frac{\partial A_2^{(1)}(r,\theta)}{\partial r}\right|_{r=R_m}\\&=-\frac{\sin(\theta-\phi)}{R_m^{\ 2}}\left[\frac{\partial A_1^{(0)}(r,\theta)}{\partial\theta}-\frac{\partial A_2^{(0)}(r,\theta)}{\partial\theta}\right]\bigg|_{r=R_m}\\&+\left.\frac{\mu_0 M_r}{R_m}\sin(\theta-\phi)\right|_{r=R_m}\\&-\cos(\theta-\phi)\left[\frac{\partial^2 A_1^{(0)}(r,\theta)}{\partial r^2}-\frac{\partial^2 A_2^{(0)}(r,\theta)}{\partial r^2}\right]\bigg|_{r=R_m}\end{aligned} \tag{30}$$

$$\begin{aligned}&\left.\frac{\partial A_1^{(1)}(r,\theta)}{\partial\theta}-\frac{\partial A_2^{(1)}(r,\theta)}{\partial\theta}\right|_{r=R_m}\\&=\sin(\theta-\phi)\left[\frac{\partial A_1^{(0)}(r,\theta)}{\partial r}-\frac{\partial A_2^{(0)}(r,\theta)}{\partial r}\right]\bigg|_{r=R_m}\\&-\cos(\theta-\phi)\left[\frac{\partial^2 A_1^{(0)}(r,\theta)}{\partial\theta\partial r}-\frac{\partial^2 A_2^{(0)}(r,\theta)}{\partial\theta\partial r}\right]\bigg|_{r=R_m}\\&+\frac{\cos(\theta-\phi)}{R_m}\left[\frac{\partial A_1^{(0)}(r,\theta)}{\partial\theta}-\frac{\partial A_2^{(0)}(r,\theta)}{\partial\theta}\right]\bigg|_{r=R_m}\end{aligned} \tag{31}$$

$$H_{\theta3,i}^{(1)}(R_s,\theta)=H_{\theta2}^{(1)}(R_s,\theta)\quad\theta\in[\theta_i,\theta_i+\beta] \tag{32}$$

$$A_{3,i}^{(1)}(R_s,\theta)=A_2^{(1)}(R_s,\theta)\quad\theta\in[\theta_i,\theta_i+\beta] \tag{33}$$

3.3 矢量磁位一阶通式

永磁区域 1 和气隙区域 2 内矢量磁位的一阶通式 $A_1^{(1)}$ 和 $A_2^{(1)}$ 为：

$$A_1^{(1)}(r,\theta)=\sum_{n=1}^{\infty}\begin{bmatrix}(A_{1n}^{(1)}r^{nm-1}+B_{1n}^{(1)}r^{-(nm-1)})\cos(nm-1)\theta\\+(C_{1n}^{(1)}r^{nm-1}+D_{1n}^{(1)}r^{-(nm-1)})\sin(nm-1)\theta\\+(E_{1n}^{(1)}r^{nm+1}+F_{1n}^{(1)}r^{-(nm+1)})\cos(nm+1)\theta\\+(G_{1n}^{(1)}r^{nm+1}+H_{1n}^{(1)}r^{-(nm+1)})\sin(nm+1)\theta\end{bmatrix} \tag{34}$$

$$A_2^{(1)}(r,\theta)=\sum_{n=1}^{\infty}\begin{bmatrix}(A_{2n}^{(1)}r^{nm-1}+B_{2n}^{(1)}r^{-(nm-1)})\cos(nm-1)\theta\\+(C_{2n}^{(1)}r^{nm-1}+D_{2n}^{(1)}r^{-(nm-1)})\sin(nm-1)\theta\\+(E_{2n}^{(1)}r^{nm+1}+F_{2n}^{(1)}r^{-(nm+1)})\cos(nm+1)\theta\\+(G_{2n}^{(1)}r^{nm+1}+H_{2n}^{(1)}r^{-(nm+1)})\sin(nm+1)\theta\end{bmatrix} \tag{35}$$

其中 $A_{1n}^{(1)}\sim H_{1n}^{(1)}$、$A_{2n}^{(1)}\sim H_{2n}^{(1)}$ 为永磁区域和气隙区域一阶通解待定系数，具体表达式见附录 A。

槽区域 3 内矢量磁位的一阶通式为：

$$A_{3,i}^{(1)}(r,\theta)=A_i^{(1)}+\sum_{k=1}^{\infty}A_{3,i}^{(1)}(k,i)\frac{(\frac{r}{R_{sy}})^{k\pi/\beta}+(\frac{r}{R_{sy}})^{-k\pi/\beta}}{(\frac{R_s}{R_{sy}})^{k\pi/\beta}+(\frac{R_s}{R_{sy}})^{-k\pi/\beta}}\cos\frac{k\pi}{\beta}(\theta-\theta_i) \tag{36}$$

其中，$A_i^{(1)}$ 和 $A_{3,i}^{(1)}(k,i)$ 为槽区域一阶通解待定

系数。

根据边界条件(29)，由傅立叶积分可得：

$$\begin{aligned}&(nm-1)(A_{2n}^{(1)}R_s^{\,nm-2}-B_{2n}^{(1)}R_s^{\,-nm})\\&=\frac{1}{\pi}\sum_{i=1}^{Q}\int_{\theta_i}^{\theta_i+\beta}\sum_{k=1}^{\infty}\alpha_k A_{3,i}^{(1)}(k,i)\cos\frac{k\pi}{\beta}(\theta-\theta_i)\cos(nm-1)\theta d\theta\end{aligned}\tag{37}$$

$$\begin{aligned}&(nm-1)(C_{2n}^{(1)}R_s^{\,nm-2}-D_{2n}^{(1)}R_s^{\,-nm})\\&=\frac{1}{\pi}\sum_{i=1}^{Q}\int_{\theta_i}^{\theta_i+\beta}\sum_{k=1}^{\infty}\alpha_k A_{3,i}^{(1)}(k,i)\cos\frac{k\pi}{\beta}(\theta-\theta_i)\sin(nm-1)\theta d\theta\end{aligned}\tag{38}$$

$$\begin{aligned}&(nm+1)(E_{2n}^{(1)}R_s^{\,nm}-F_{2n}^{(1)}R_s^{\,-nm-2})\\&=\frac{1}{\pi}\sum_{i=1}^{Q}\int_{\theta_i}^{\theta_i+\beta}\sum_{k=1}^{\infty}\alpha_k A_{3,i}^{(1)}(k,i)\cos\frac{k\pi}{\beta}(\theta-\theta_i)\cos(nm+1)\theta d\theta\end{aligned}\tag{39}$$

$$\begin{aligned}&(nm+1)(G_{2n}^{(1)}R_s^{\,nm}-H_{2n}^{(1)}R_s^{\,-nm-2})\\&=\frac{1}{\pi}\sum_{i=1}^{Q}\int_{\theta_i}^{\theta_i+\beta}\sum_{k=1}^{\infty}\alpha_k A_{3,i}^{(1)}(k,i)\cos\frac{k\pi}{\beta}(\theta-\theta_i)\sin(nm+1)\theta d\theta\end{aligned}\tag{40}$$

式中：

$$\alpha_k=\frac{k\pi}{\beta R_{sy}}\frac{(\frac{R_s}{R_{sy}})^{k\pi/\beta-1}-(\frac{R_s}{R_{sy}})^{-k\pi/\beta-1}}{(\frac{R_s}{R_{sy}})^{k\pi/\beta}+(\frac{R_s}{R_{sy}})^{-k\pi/\beta}}\tag{41}$$

根据边界条件(30)，由傅立叶积分可得：

$$\begin{aligned}&A_{3,i}^{(1)}(k,i)=\frac{2}{\beta}\int_{\theta_i}^{\theta_i+\beta}A_2^{(1)}(R_s,\theta)\cos\frac{k\pi}{\beta}(\theta-\theta_i)d\theta\\&=\frac{2}{\beta}\int_{\theta_i}^{\theta_i+\beta}\sum_{n=1}^{\infty}\begin{bmatrix}(A_{2n}^{(1)}R_s^{\,nm-1}+B_{2n}^{(1)}R_s^{\,-(nm-1)})\cos(nm-1)\theta\\+(C_{2n}^{(1)}R_s^{\,nm-1}+D_{2n}^{(1)}R_s^{\,-(nm-1)})\sin(nm-1)\theta\\+(E_{2n}^{(1)}R_s^{\,nm+1}+F_{2n}^{(1)}R_s^{\,-(nm+1)})\cos(nm+1)\theta\\+(G_{2n}^{(1)}R_s^{\,nm+1}+H_{2n}^{(1)}R_s^{\,-(nm+1)})\sin(nm+1)\theta\end{bmatrix}\cos\frac{k\pi}{\beta}(\theta-\theta_i)d\theta\end{aligned}\tag{42}$$

联立以上一阶边界条件，求取各区域矢量磁位一阶通解待定系数后，根据式(10)可求得气隙磁通密度一阶分量。

4　磁通密度、不平衡磁拉力和齿槽转矩

4.1 磁通密度

表贴式永磁电机转子偏心气隙磁密由零阶分量和一阶分量组成：

$$B_{r2}(r,\theta)=B_{r2}^{(0)}(r,\theta)+\varepsilon B_{r2}^{(1)}(r,\theta)\tag{43}$$

$$B_{\theta 2}(r,\theta)=B_{\theta 2}^{(0)}(r,\theta)+\varepsilon B_{\theta 2}^{(1)}(r,\theta)\tag{44}$$

其中， B_{r2} 和 $B_{\theta 2}$ 分别为转子偏心后气隙磁密的径向和切向分量。

4.2 不平衡磁拉力和齿槽转矩

由麦克斯韦应力张量法，气隙内某一点所受径向和切向磁拉力可表示为：

$$f_r=\frac{1}{2\mu_0}\left(B_{r2}^2-B_{\theta 2}^2\right)\cos\theta\tag{45}$$

$$f_\theta=\frac{1}{\mu_0}B_{r2}B_{\theta 2}\tag{46}$$

那么，根据坐标变换，沿一圆周路径积分，可求得 x 和 y 方向上，转子所受不平衡磁拉力为[3]：

$$\begin{aligned}F_x&=\int_0^{L_{ef}}\int_0^{2\pi}f_x r_g d\theta dz\\&=L_{ef}r_g\int_0^{2\pi}[\frac{1}{2\mu_0}\left(B_{r2}^2-B_{\theta 2}^2\right)\cos\theta-\frac{1}{\mu_0}(B_{r2}B_{\theta 2})\sin\theta]d\theta\end{aligned}\tag{47}$$

$$\begin{aligned}F_y&=\int_0^{L_{ef}}\int_0^{2\pi}f_y r_g d\theta dz\\&=L_{ef}r_g\int_0^{2\pi}[\frac{1}{2\mu_0}\left(B_{r2}^2-B_{\theta 2}^2\right)\sin\theta+\frac{1}{\mu_0}B_{r2}B_{\theta 2}\cos\theta]d\theta\end{aligned}\tag{48}$$

齿槽转矩表达式：

$$T_{\mathrm{cog}}=\frac{L_{\mathrm{ef}}r_{\mathrm{g}}^{\,2}}{\mu_0}\int_0^{2\pi}B_{\mathrm{r2}}B_{\mathrm{\theta 2}}d\theta\tag{49}$$

其中，L_{ef} 为轴向长度，r_{g} 为积分半径。

5　有限元分析比较

为验证解析模型的合理性，本文使用 Jmag 有限元分析软件，建立 8 极 12 槽表贴式永磁电机偏心模型，将气隙磁通密度、齿槽转矩和不平衡磁拉力有限元分析结果与解析结果作对比。模型参数如表 1 所示。

表 1　电机模型参数

Tab.1　Prototype parameters

符号	参数名称	取值
R_{r}	转子半径	26 mm
$\mathrm{h_m}$	永磁体厚度	4 mm
g	气隙厚度	1 mm
R_{sy}	定子槽低半径	40 mm
L_{ef}	轴向长度	20 mm
p	极对数	4
Q	定子槽数	12
B_{r}	永磁体剩磁	1.1 T
μ_0	空气磁导率	4πe-7 N/A^2
β	槽口角度	0.1571 rad
$n_{\max}$	永磁体区域和气隙区域傅立叶展开次数	360
$k_{\max}$	槽区域傅立叶展开次数	60

图 2 所示为定转子同心时，以 r=30.75mm 提取的气隙磁密波形，解析结果和有限元结果的对比。其中，实线和虚线分别代表气隙磁密解析解的径向和切向分量，“*”和“.”分别代表气隙磁密有限元解的径向和切向分量。

图 3 所示为转子偏心角度 $\phi=0$，转子偏心量 ε 分别取 0.3g、0.5g 和 0.8g 时，气隙磁密一阶分量 $\varepsilon B_{r2}^{(1)}$ 和 $\varepsilon B_{\theta 2}^{(1)}$ 的解析解波形。图中可见，偏心量 ε 越大，气隙磁密一阶分量越大，即波形畸变程度越大。

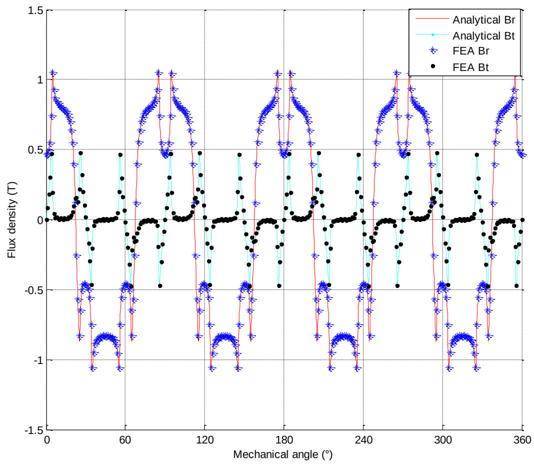

图 2 定转子同心时气隙磁密波形比较

Fig. 2 Comparison between FEA and Analytical results of the air-gap flux density without rotor eccentricity

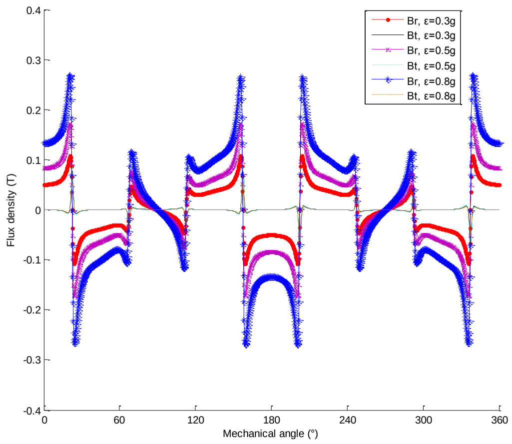

图 3 不同转子偏心量下气隙磁密一阶分量波形

Fig. 3 Waveforms of the air-gap flux density under different *ε*

图 4 为转子偏心角度 $\phi=0$，转子偏心量 ε=0.5g 时，偏心气隙磁密波形的解析解与有限元解比较。由图可见，解析解与有限元解的趋势一致。

图 5 为转子偏心角度 $\phi=0$，转子偏心量 ε=0.5g 时，齿槽转矩解析结果与有限元结果对比。其中，实线表示解析计算所得齿槽转矩，“。”代表有限元计算所得齿槽转矩。

使转子偏心角度 ϕ 由 $0\sim360^\circ$ 变化，转子偏心量 ε 维持在 0.5g，将偏心转子受到的不平衡磁拉力描绘成曲线，如图 6 所示。其中，实现和虚线分别代表 x 轴方向不平衡磁拉力 F_x 和 y 轴方向不平衡磁拉力 F_y 的解析波形，“。”和“*”分别代表 F_x 和 F_y 的有限元分析波形。

6 结论

本文建立了定子开槽表贴式永磁电机转子偏心气隙磁场全局解析模型，通过矢量磁位计算，给出偏心气隙区域待定系数表达式，物理概念明晰。通过与有限元分析结果的比较，气隙磁密、齿槽转矩以及不平衡磁拉力的解析解与有限元解趋势一致，验证了全局解析法的合理性。为永磁电机转子偏心磁场性能研究提供了有效的工具。

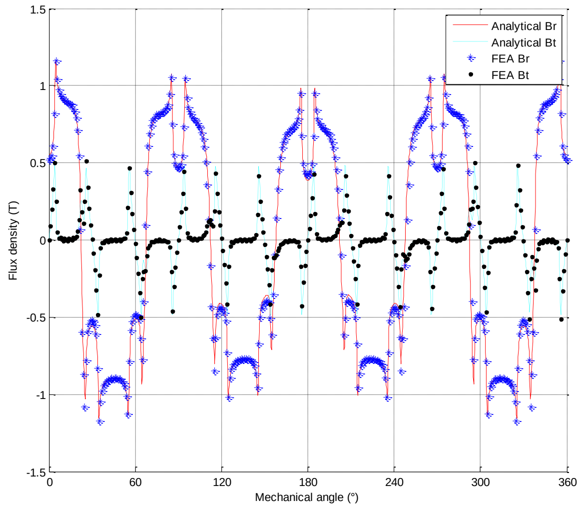

图 4 $\phi=0$ 且 ε=0.5g 时偏心气隙磁通密度波形比较

Fig. 4 Comparison between FEA and Analytical results of the air-gap flux density with $\phi=0$ and ε=0.5g

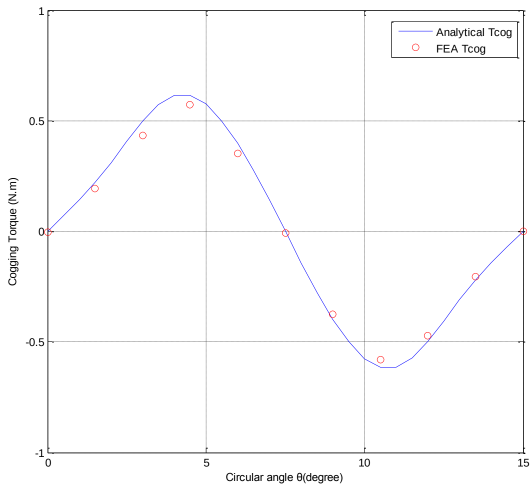

图 5 $\phi=0$ 且 ε=0.5g 时齿槽转矩波形比较

Fig. 5 Comparison between FEA and Analytical results of cogging torque waveforms with $\phi=0$ and ε=0.5g

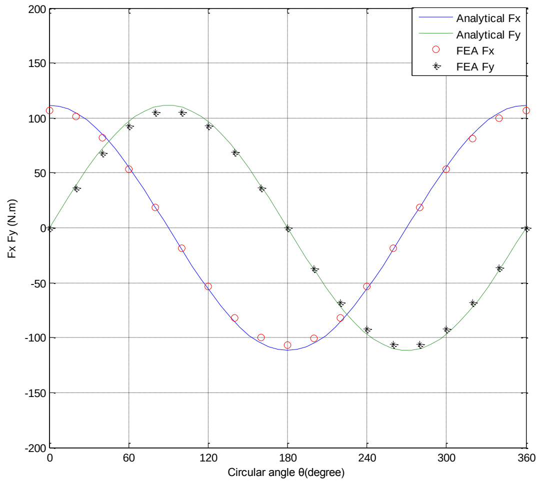

图 6　$\phi=0\sim360^{\circ}$ 且 ε=0.5g 时不平衡磁拉力波形比较

Fig. 6　Comparison between FEA and Analytical results of unbalanced magnetic forces waveforms with $\phi=0\sim360^{\circ}$ **and** ε=0.5g

附录 A

一阶方程气隙区域待定系数表达式：

$$
\left.\begin{aligned}
A_{2n}^{(1)} &= \frac{R_s^{nm-1}}{R_s^{2nm-2}-R_r^{2nm-2}}a_n + L_{an}\\
B_{2n}^{(1)} &= \frac{R_s^{nm-1}R_r^{2nm-2}}{R_s^{2nm-2}-R_r^{2nm-2}}a_n + L_{bn}\\
C_{2n}^{(1)} &= \frac{R_s^{nm-1}}{R_s^{2nm-2}-R_r^{2nm-2}}b_n + L_{cn}\\
D_{2n}^{(1)} &= \frac{R_s^{nm-1}R_r^{2nm-2}}{R_s^{2nm-2}-R_r^{2nm-2}}b_n + L_{dn}
\end{aligned}\right\} \tag{A1}
$$

$$
\left.\begin{aligned}
E_{2n}^{(1)} &= \frac{R_s^{nm+1}}{R_s^{2nm+2}-R_r^{2nm+2}}c_n + L_{en}\\
F_{2n}^{(1)} &= \frac{R_s^{nm+1}R_r^{2nm+2}}{R_s^{2nm+2}-R_r^{2nm+2}}c_n + L_{fn}\\
G_{2n}^{(1)} &= \frac{R_s^{nm+1}}{R_s^{2nm+2}-R_r^{2nm+2}}d_n + L_{gn}\\
H_{2n}^{(1)} &= \frac{R_s^{nm+1}R_r^{2nm+2}}{R_s^{2nm+2}-R_r^{2nm+2}}d_n + L_{hn}
\end{aligned}\right\} \tag{A2}
$$

以上各式中：

$$
\begin{aligned}
L_{an} = {}& \frac{-R_r^{nm}\rho_{1n}}{R_s^{2nm-2}-R_r^{2nm-2}} + \frac{(R_m^{-nm+2}R_r^{2nm-2}+R_m^{nm})\varsigma_{1n}}{2(R_s^{2nm-2}-R_r^{2nm-2})}\\
&+\frac{(R_m^{-nm}R_r^{2nm-2}-R_m^{nm-2})\zeta_{1n}}{2(R_s^{2nm-2}-R_r^{2nm-2})}
\end{aligned} \tag{A3}
$$

$$
\begin{aligned}
L_{bn} = {}& \frac{-R_s^{2nm-2}R_r^{nm}\rho_{1n}}{R_s^{2nm-2}-R_r^{2nm-2}} + \frac{R_s^{2nm-2}(R_m^{-nm+2}R_r^{2nm-2}+R_m^{nm})\varsigma_{1n}}{2(R_s^{2nm-2}-R_r^{2nm-2})}\\
&+\frac{R_s^{2nm-2}(R_m^{-nm}R_r^{2nm-2}-R_m^{nm-2})\zeta_{1n}}{2(R_s^{2nm-2}-R_r^{2nm-2})}
\end{aligned} \tag{A4}
$$

$$
\begin{aligned}
L_{cn} = {}& \frac{-R_r^{nm}\rho_{2n}}{R_s^{2nm-2}-R_r^{2nm-2}} + \frac{(R_m^{-nm+2}R_r^{2nm-2}+R_m^{nm})\varsigma_{2n}}{2(R_s^{2nm-2}-R_r^{2nm-2})}\\
&+\frac{(R_m^{-nm}R_r^{2nm-2}-R_m^{nm-2})\zeta_{2n}}{2(R_s^{2nm-2}-R_r^{2nm-2})}
\end{aligned} \tag{A5}
$$

$$
\begin{aligned}
L_{dn} = {}& \frac{-R_s^{2nm-2}R_r^{nm}\rho_{2n}}{R_s^{2nm-2}-R_r^{2nm-2}} + \frac{R_s^{2nm-2}(R_m^{-nm+2}R_r^{2nm-2}+R_m^{nm})\varsigma_{2n}}{2(R_s^{2nm-2}-R_r^{2nm-2})}\\
&+\frac{R_s^{2nm-2}(R_m^{-nm}R_r^{2nm-2}-R_m^{nm-2})\zeta_{2n}}{2(R_s^{2nm-2}-R_r^{2nm-2})}
\end{aligned} \tag{A6}
$$

$$
\begin{aligned}
L_{en} = {}& \frac{-R_r^{nm+2}\rho_{3n}}{R_s^{2nm+2}-R_r^{2nm+2}} + \frac{(R_r^{2nm+2}R_m^{-nm}+R_m^{nm+2})\varsigma_{3n}}{2(R_s^{2nm+2}-R_r^{2nm+2})}\\
&+\frac{(R_r^{2nm+2}R_m^{-nm-2}-R_m^{nm})\zeta_{3n}}{2(R_s^{2nm+2}-R_r^{2nm+2})}
\end{aligned} \tag{A7}
$$

$$
\begin{aligned}
L_{fn} = {}& \frac{-R_s^{2nm+2}R_r^{nm+2}\rho_{3n}}{R_s^{2nm+2}-R_r^{2nm+2}} + \frac{R_s^{2nm+2}(R_r^{2nm+2}R_m^{-nm}+R_m^{nm+2})\varsigma_{3n}}{2(R_s^{2nm+2}-R_r^{2nm+2})}\\
&+\frac{R_s^{2nm+2}(R_r^{2nm+2}R_m^{-nm-2}-R_m^{nm})\zeta_{3n}}{2(R_s^{2nm+2}-R_r^{2nm+2})}
\end{aligned} \tag{A8}
$$

$$
\begin{aligned}
L_{gn} = {}& \frac{-R_r^{nm+2}\rho_{4n}}{R_s^{2nm+2}-R_r^{2nm+2}} + \frac{(R_r^{2nm+2}R_m^{-nm}+R_m^{nm+2})\varsigma_{4n}}{2(R_s^{2nm+2}-R_r^{2nm+2})}\\
&+\frac{(R_r^{2nm+2}R_m^{-nm-2}-R_m^{nm})\zeta_{4n}}{2(R_s^{2nm+2}-R_r^{2nm+2})}
\end{aligned} \tag{A9}
$$

$$
\begin{aligned}
L_{hn} = {}& \frac{-R_s^{2nm+2}R_r^{nm+2}\rho_{4n}}{R_s^{2nm+2}-R_r^{2nm+2}} + \frac{R_s^{2nm+2}(R_r^{2nm+2}R_m^{-nm}+R_m^{nm+2})\varsigma_{4n}}{2(R_s^{2nm+2}-R_r^{2nm+2})}\\
&+\frac{R_s^{2nm+2}(R_r^{2nm+2}R_m^{-nm-2}-R_m^{nm})\zeta_{4n}}{2(R_s^{2nm+2}-R_r^{2nm+2})}
\end{aligned} \tag{A10}
$$

其中：

$$
\begin{aligned}
\rho_{1n} = {}& -\frac{1}{2(nm-1)}\\
&\left\{\begin{aligned}
&[nm(nm-2)R_r^{nm-2}A_{1n}^{(0)}+(nm)^2R_r^{-nm-2}B_{1n}^{(0)}+\frac{\mu_0 M_n\sin nm\theta_0}{R_r[(nm)^2-1]}]\cos\phi\\
&+[nm(nm-2)R_r^{nm-2}C_{1n}^{(0)}+(nm)^2R_r^{-nm-2}D_{1n}^{(0)}-\frac{\mu_0 M_n\cos nm\theta_0}{R_r[(nm)^2-1]}]\sin\phi
\end{aligned}\right\}
\end{aligned} \tag{A11}
$$

$$
\begin{aligned}
\rho_{2n} = {}& \frac{1}{2(nm-1)}\\
&\left\{\begin{aligned}
&[nm(nm-2)R_r^{nm-2}A_{1n}^{(0)}+(nm)^2R_r^{-nm-2}B_{1n}^{(0)}+\frac{\mu_0 M_n\sin nm\theta_0}{R_r[(nm)^2-1]}]\sin\phi\\
&-[nm(nm-2)R_r^{nm-2}C_{1n}^{(0)}+(nm)^2R_r^{-nm-2}D_{1n}^{(0)}-\frac{\mu_0 M_n\cos nm\theta_0}{R_r[(nm)^2-1]}]\cos\phi
\end{aligned}\right\}
\end{aligned} \tag{A12}
$$

$$
\begin{aligned}
\rho_{3n} = {}& -\frac{1}{2(nm+1)}\\
&\left\{\begin{aligned}
&[(nm)^2R_r^{nm-2}A_{1n}^{(0)}+nm(nm+2)R_r^{-nm-2}B_{1n}^{(0)}-\frac{\mu_0 M_n\sin nm\theta_0}{R_r[(nm)^2-1]}]\cos\phi\\
&-[(nm)^2R_r^{nm-2}C_{1n}^{(0)}+nm(nm+2)R_r^{-nm-2}D_{1n}^{(0)}+\frac{\mu_0 M_n\cos nm\theta_0}{R_r[(nm)^2-1]}]\sin\phi
\end{aligned}\right\}
\end{aligned} \tag{A13}
$$

$$
\begin{aligned}
\rho_{4n} = {}& -\frac{1}{2(nm+1)}\\
&\left\{\begin{aligned}
&[(nm)^2R_r^{nm-2}A_{1n}^{(0)}+nm(nm+2)R_r^{-nm-2}B_{1n}^{(0)}-\frac{\mu_0 M_n\sin nm\theta_0}{R_r[(nm)^2-1]}]\sin\phi\\
&+[(nm)^2R_r^{nm-2}C_{1n}^{(0)}+nm(nm+2)R_r^{-nm-2}D_{1n}^{(0)}+\frac{\mu_0 M_n\cos nm\theta_0}{R_r[(nm)^2-1]}]\cos\phi
\end{aligned}\right\}
\end{aligned} \tag{A14}
$$

$$\varsigma_{1n}=-\frac{1}{2(nm-1)}\left\{\begin{array}{l}\left[\begin{array}{l}nm(nm-2)R_m^{\;nm-2}A_{1n}^{(0)}+(nm)^2R_m^{\;-nm-2}B_{1n}^{(0)}\\ -nm(nm-2)R_m^{\;nm-2}A_{2n}^{(0)}-(nm)^2R_m^{\;-nm-2}B_{2n}^{(0)}+\dfrac{\mu_0M_n\sin nm\theta_0}{R_m[(nm)^2-1]}\end{array}\right]\cos\phi\\ +\left[\begin{array}{l}nm(nm-2)R_m^{\;nm-2}C_{1n}^{(0)}+(nm)^2R_m^{\;-nm-2}D_{1n}^{(0)}\\ -nm(nm-2)R_m^{\;nm-2}C_{2n}^{(0)}-(nm)^2R_m^{\;-nm-2}D_{2n}^{(0)}-\dfrac{\mu_0M_n\cos nm\theta_0}{R_m[(nm)^2-1]}\end{array}\right]\sin\phi\end{array}\right\}\tag{A15}$$

$$\varsigma_{2n}=\frac{1}{2(nm-1)}\left\{\begin{array}{l}\left[\begin{array}{l}nm(nm-2)R_m^{\;nm-2}A_{1n}^{(0)}+(nm)^2R_m^{\;-nm-2}B_{1n}^{(0)}\\ -nm(nm-2)R_m^{\;nm-2}A_{2n}^{(0)}-(nm)^2R_m^{\;-nm-2}B_{2n}^{(0)}+\dfrac{\mu_0M_n\sin nm\theta_0}{R_m[(nm)^2-1]}\end{array}\right]\sin\phi\\ -\left[\begin{array}{l}nm(nm-2)R_m^{\;nm-2}C_{1n}^{(0)}+(nm)^2R_m^{\;-nm-2}D_{1n}^{(0)}\\ -nm(nm-2)R_m^{\;nm-2}C_{2n}^{(0)}-(nm)^2R_m^{\;-nm-2}D_{2n}^{(0)}-\dfrac{\mu_0M_n\cos nm\theta_0}{R_m[(nm)^2-1]}\end{array}\right]\cos\phi\end{array}\right\}\tag{A16}$$

$$\varsigma_{3n}=-\frac{1}{2(nm+1)}\left\{\begin{array}{l}\left[\begin{array}{l}(nm)^2R_m^{\;nm-2}A_{1n}^{(0)}+nm(nm+2)R_m^{\;-nm-2}B_{1n}^{(0)}\\ -(nm)^2R_m^{\;nm-2}A_{2n}^{(0)}-nm(nm+2)R_m^{\;-nm-2}B_{2n}^{(0)}-\dfrac{\mu_0M_n\sin nm\theta_0}{R_m[(nm)^2-1]}\end{array}\right]\cos\phi\\ -\left[\begin{array}{l}(nm)^2R_m^{\;nm-2}C_{1n}^{(0)}+nm(nm+2)R_m^{\;-nm-2}D_{1n}^{(0)}\\ -(nm)^2R_m^{\;nm-2}C_{2n}^{(0)}-nm(nm+2)R_m^{\;-nm-2}D_{2n}^{(0)}+\dfrac{\mu_0M_n\cos nm\theta_0}{R_m[(nm)^2-1]}\end{array}\right]\sin\phi\end{array}\right\}\tag{A17}$$

$$\varsigma_{4n}=-\frac{1}{2(nm+1)}\left\{\begin{array}{l}\left[\begin{array}{l}(nm)^2R_m^{\;nm-2}A_{1n}^{(0)}+nm(nm+2)R_m^{\;-nm-2}B_{1n}^{(0)}\\ -(nm)^2R_m^{\;nm-2}A_{2n}^{(0)}-nm(nm+2)R_m^{\;-nm-2}B_{2n}^{(0)}-\dfrac{\mu_0M_n\sin nm\theta_0}{R_m[(nm)^2-1]}\end{array}\right]\sin\phi\\ +\left[\begin{array}{l}(nm)^2R_m^{\;nm-2}C_{1n}^{(0)}+nm(nm+2)R_m^{\;-nm-2}D_{1n}^{(0)}\\ -(nm)^2R_m^{\;nm-2}C_{2n}^{(0)}-nm(nm+2)R_m^{\;-nm-2}D_{2n}^{(0)}+\dfrac{\mu_0M_n\cos nm\theta_0}{R_m[(nm)^2-1]}\end{array}\right]\cos\phi\end{array}\right\}\tag{A18}$$

$$\zeta_{1n}=-\frac{1}{2(nm-1)}\left\{\begin{array}{l}\left[\begin{array}{l}nm(nm-2)A_{1n}^{(0)}R_m^{\;nm}-(nm)^2R_m^{\;-nm}B_{1n}^{(0)}\\ -nm(nm-2)R_m^{\;nm}A_{2n}^{(0)}+(nm)^2R_m^{\;-nm}B_{2n}^{(0)}+\dfrac{\mu_0M_nnmR_m\sin nm\theta_0}{(nm)^2-1}\end{array}\right]\cos\phi\\ +\left[\begin{array}{l}nm(nm-2)C_{1n}^{(0)}R_m^{\;nm}-(nm)^2R_m^{\;-nm}D_{1n}^{(0)}\\ -nm(nm-2)R_m^{\;nm}C_{2n}^{(0)}+(nm)^2R_m^{\;-nm}D_{2n}^{(0)}-\dfrac{\mu_0M_nnmR_m\cos nm\theta_0}{(nm)^2-1}\end{array}\right]\sin\phi\end{array}\right\}\tag{A19}$$

$$\zeta_{2n}=\frac{1}{2(nm-1)}\left\{\begin{array}{l}\left[\begin{array}{l}nm(nm-2)A_{1n}^{(0)}R_m^{\;nm}-(nm)^2R_m^{\;-nm}B_{1n}^{(0)}\\ -nm(nm-2)R_m^{\;nm}A_{2n}^{(0)}+(nm)^2R_m^{\;-nm}B_{2n}^{(0)}+\dfrac{\mu_0M_nnmR_m\sin nm\theta_0}{(nm)^2-1}\end{array}\right]\sin\phi\\ -\left[\begin{array}{l}nm(nm-2)C_{1n}^{(0)}R_m^{\;nm}-(nm)^2R_m^{\;-nm}D_{1n}^{(0)}\\ -nm(nm-2)R_m^{\;nm}C_{2n}^{(0)}+(nm)^2R_m^{\;-nm}D_{2n}^{(0)}-\dfrac{\mu_0M_nnmR_m\cos nm\theta_0}{(nm)^2-1}\end{array}\right]\cos\phi\end{array}\right\}\tag{A20}$$

$$\zeta_{3n}=-\frac{1}{2(nm+1)}\left\{\begin{array}{l}\left[\begin{array}{l}(nm)^2R_m^{\;nm}A_{1n}^{(0)}-nm(nm+2)R_m^{\;-nm}B_{1n}^{(0)}\\ -(nm)^2R_m^{\;nm}A_{2n}^{(0)}+nm(nm+2)R_m^{\;-nm}B_{2n}^{(0)}-\dfrac{\mu_0M_nnmR_m\sin nm\theta_0}{(nm)^2-1}\end{array}\right]\cos\phi\\ -\left[\begin{array}{l}(nm)^2R_m^{\;nm}C_{1n}^{(0)}-nm(nm+2)R_m^{\;-nm}D_{1n}^{(0)}\\ -(nm)^2R_m^{\;nm}C_{2n}^{(0)}+nm(nm+2)R_m^{\;-nm}D_{2n}^{(0)}+\dfrac{\mu_0M_nnmR_m\cos nm\theta_0}{(nm)^2-1}\end{array}\right]\sin\phi\end{array}\right\}\tag{A21}$$

$$\zeta_{4n}=-\frac{1}{2(nm+1)}\left\{\begin{array}{l}\left[\begin{array}{l}(nm)^2R_m^{\;nm}A_{1n}^{(0)}-nm(nm+2)R_m^{\;-nm}B_{1n}^{(0)}\\ -(nm)^2R_m^{\;nm}A_{2n}^{(0)}+nm(nm+2)R_m^{\;-nm}B_{2n}^{(0)}-\dfrac{\mu_0M_nnmR_m\sin nm\theta_0}{(nm)^2-1}\end{array}\right]\sin\phi\\ +\left[\begin{array}{l}(nm)^2R_m^{\;nm}C_{1n}^{(0)}-nm(nm+2)R_m^{\;-nm}D_{1n}^{(0)}\\ -(nm)^2R_m^{\;nm}C_{2n}^{(0)}+nm(nm+2)R_m^{\;-nm}D_{2n}^{(0)}+\dfrac{\mu_0M_nnmR_m\cos nm\theta_0}{(nm)^2-1}\end{array}\right]\cos\phi\end{array}\right\}\tag{A22}$$

$$\begin{aligned}a_n&=\frac{R_s}{\pi(nm-1)}\sum_{i=1}^{Q}\sum_{k=1}^{\infty}\alpha_kA_{3,i}^{(1)}(k,i)\cdot p_k^i(n)\\ b_n&=\frac{R_s}{\pi(nm-1)}\sum_{i=1}^{Q}\sum_{k=1}^{\infty}\alpha_kA_{3,i}^{(1)}(k,i)\cdot q_k^i(n)\\ c_n&=\frac{R_s}{\pi(nm+1)}\sum_{i=1}^{Q}\sum_{k=1}^{\infty}\alpha_kA_{3,i}^{(1)}(k,i)\cdot s_k^i(n)\\ d_n&=\frac{R_s}{\pi(nm+1)}\sum_{i=1}^{Q}\sum_{k=1}^{\infty}\alpha_kA_{3,i}^{(1)}(k,i)\cdot t_k^i(n)\end{aligned}\tag{A23}$$

$$\begin{aligned}p_k^i(n)&=\int_{\theta_i}^{\theta_i+\beta}\cos\frac{k\pi}{\beta}(\theta-\theta_i)\cos(nm-1)\theta d\theta\\ q_k^i(n)&=\int_{\theta_i}^{\theta_i+\beta}\cos\frac{k\pi}{\beta}(\theta-\theta_i)\sin(nm-1)\theta d\theta\\ s_k^i(n)&=\int_{\theta_i}^{\theta_i+\beta}\cos\frac{k\pi}{\beta}(\theta-\theta_i)\cos(nm+1)\theta d\theta\\ t_k^i(n)&=\int_{\theta_i}^{\theta_i+\beta}\cos\frac{k\pi}{\beta}(\theta-\theta_i)\sin(nm+1)\theta d\theta\end{aligned}\tag{A24}$$

参考文献

[1] U. Kim and D. K. Lieu, Magnetic field calculation in permanent magnet motors with rotor eccentricity: Without slotting effect [J], IEEE Transactions on Magnetics, 1998, 34(4): 2243–2252.

[2] A. Rahideh and T. Korakianitis, Analytical open-circuit magnetic field distribution of slotless brushless permanent-magnet machines with rotor eccentricity [J], 2011, 47(125): 4791–4808.

[3] 仇志坚，李琛，周晓燕等. 表贴式永磁电机转子偏心空载气隙磁场解析[J]. 电工技术学报,2013, 28(3)：114-121.
Qiu Zhijian, Li Chen, Zhou Xiaoyan, et al．Analytical calculation of no-load air-gap magnetic field in surface-mounted permanent magnet motors with rotor eccentricity[J]．Transactions of China Electro-technical Society,2013, 28(3) ：114-121 (in Chinese).

[4] 张冉，王秀和等. 基于等效剩磁法的永磁电动机转子偏心磁场解析计算[J]. 电工技术学报，2009，24(5)：7-12.
Zhang ran，Wang Xiuhe，et al. Analytical prediction of magnetic field in permanent magnet motors with rotor eccentricity based on the method of equivalent remanence [J]. Transactions of China electrotechnical society，2009，24(5)：7-12 (in Chinese).

[5] U. Kim and D. K. Lieu, Magnetic field calculation in permanent magnet motors with rotor eccentricity: With slotting effect considered [J], IEEE Transactions on Magnetics, 1998, 34(4): 2253–2266.

[6] U. Kim and D. K. Lieu, Effects of magnetically induced vibration force in brushless permanent-magnet motors [J], IEEE Transactions on Magnetics, 2005,41(6): 2164–2172.

[7] J. T. Li, Z. J. Liu, and L. H. A. Nay, Effect of Radial Magnetic Forces in Permanent Magnet Motors With Rotor Eccentricity [J], IEEE Transactions on Magnetics, 2007,43(6): 2525–2527.

[8] Jiajing Fu and Changsheng Zhu, Subdomain model for predicting magnetic field in slotted surface mounted permanent-magnet

machines with rotor eccentricity [J], IEEE Transactions on Magnetics, 2012, 48(5): 1906–1917.

[9] 李节宝，井立兵，周晓燕等. 表贴式永磁无刷电机直接解析计算方法[J]. 电工技术学报, 2012, 27(11): 83-88.
Li Jiebao, Jing Libing, Zhou Xiaoyan, Zhang Yuejin. Exact Analytical Method for Surface-Mounted Permanent-Magnet Brushless Motors[J], Transactions of China Electrotechnical Society, 2012, 27(11): 83-88. (in chinese)

[10] 胡之光等. 电机电磁场的分析与计算[M]. 北京：机械工业出版社, 1986: 46-47.

收稿日期：2013-07-12

基金项目：国家自然科学基金重点资助项目（51177097）。

作者简介：李　琛(1989—)，男，博士生在读，研究方向为永磁电机设计及其磁场解析；
章跃进(1956—)，男，博士，教授，博导，研究方向为电机理论、电机电磁场和电机动态仿真；
周晓燕(1978—)，女，博士生在读，主要研究方向为永磁电机设计及电机电磁场仿真；
仇志坚(1977—)，男，博士，讲师，主要研究方向为无轴承永磁同步电机研究及其控制。

通讯作者：李　琛